

Finite State Automata Inside Transformers with Chain-of-Thought: A Mechanistic Study on State Tracking

Yifan Zhang^{1,2*}, Wenyu Du³, Dongming Jin^{1,2}, Jie Fu^{4†}, Zhi Jin^{1,2†}

¹Key Laboratory of High Confidence Software Technology (PKU), MOE, China

²School of Computer Science, Peking University, China

³The University of Hong Kong, ⁴Shanghai AI Lab

yifanzhang@stu.pku.edu.cn, fujie@pjlab.org.cn, zhijin@pku.edu.cn

Abstract

Chain-of-Thought (CoT) significantly enhances the performance of large language models (LLMs) across a wide range of tasks, and prior research shows that CoT can theoretically increase expressiveness. However, there is limited mechanistic understanding of the algorithms that Transformer+CoT can learn. In this work, we (1) evaluate the state tracking capabilities of Transformer+CoT and its variants, confirming the effectiveness of CoT. (2) Next, we identify the circuit—a subset of model components—responsible for tracking the world state, finding that late-layer MLP neurons play a key role. We propose two metrics, compression and distinction, and show that the neuron sets for each state achieve nearly 100% accuracy, providing evidence of an implicit finite state automaton (FSA) embedded within the model. (3) Additionally, we explore three realistic settings: skipping intermediate steps, introducing data noise, and testing length generalization. Our results demonstrate that Transformer+CoT learns robust algorithms (FSA), highlighting its resilience in challenging scenarios.

1 Introduction

Transformer-based large language models (LLMs) Touvron et al., 2023; OpenAI, 2023 revolutionize natural language processing (NLP) by demonstrating significant progress across various tasks. However, they still face challenges with basic calculations (Zhou et al., 2023), complex reasoning (Valmeekam et al., 2024; Han et al., 2024), and regular languages (Bhattamishra et al., 2020). Approaches such as Chain-of-Thought (CoT) prompting (Wei et al., 2023) and scratchpads (Nye et al., 2021) address these limitations by generating intermediate reasoning steps. To understand the success of CoT, prior work has analyzed its expressiveness through the lenses of formal language theory

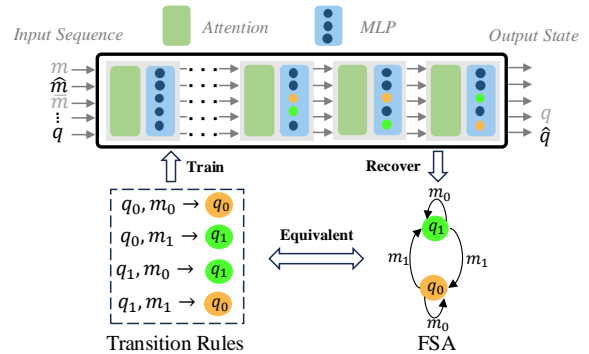


Figure 1: An illustration of one of the simplest state tracking problems, \mathbb{Z}_2 . After training on data generated by transition rules of \mathbb{Z}_2 , Transformer+CoT successfully recovers an implicit FSA by differentiating two states (q_0 and q_1) of the \mathbb{Z}_2 using two distinct sets of neurons in late-layer MLPs.

and circuit complexity. Theoretical work (Zhang et al., 2024; Qiu et al., 2024; Li et al., 2024) demonstrates that incorporating a linear number of intermediate steps increases the expressive power of log-precision transformers¹ (Merrill, William and Sabharwal, Ashish, 2024), enabling them to represent all **Finite State Automata (FSA)**, which are a foundational class of automata.

However, theoretical expressiveness indicates only upper and lower bounds on what an architecture can express; it does not guarantee successful learning during training. For instance, while recurrent neural networks (RNNs) are theoretically more expressive than transformers in Chomsky’s computational hierarchy—where RNNs can handle regular languages and transformers are positioned lower (Delétang et al., 2023)—RNNs often fail to outperform transformers in practice. Consequently, some studies investigate the expressiveness of these architectures through the lens of learnability by measuring performance in language modeling. For

*Work done during internship at Shanghai AI Lab.

†Corresponding author.

¹This paper refers to log-precision transformers; for simplicity, it uses “transformers” interchangeably.

example, Liu et al. (2023a) demonstrated that training transformers with recency-biased scratchpads improves sequential accuracy. However, even near-perfect next-token prediction accuracy does not imply that generative models reconstruct a true world model (Vafa et al., 2024). This raises a critical question: **Does CoT help Transformer recover a world model in the form of FSA, or do they merely learn shortcuts?**

To address this question, we extend the study of learnability beyond accuracy improvements, performing an internal mechanistic analysis of CoT’s success. Specifically, we focus on *state tracking*, a standard task for evaluating expressiveness (Merrill et al., 2024). In state tracking, a sequence of updates modifies the world state, which is represented as an FSA. The goal is to determine the final state after applying all updates sequentially. State tracking is a core capability of generative models and underpins many downstream tasks—such as entity tracking (Kim and Schuster, 2023), chess (Toshniwal et al., 2022), and map navigation (Liu et al., 2023b). Figure 1 illustrates \mathbb{Z}_2^2 , one of the simplest state tracking problems, along with its corresponding FSA and transition rules.

We begin by comprehensively evaluating the state tracking capabilities of Transformer+CoT, comparing it with other models (RNNs), transformer variants (e.g., those with recurrence (Fan et al., 2021; Yang et al., 2022)), and CoT variants (e.g., implicit CoT (Goyal et al., 2024)). Empirically, we show that Transformer+CoT is the only model capable of efficiently learning state tracking for sequences of arbitrary lengths across three groups: \mathbb{Z}_{60} , $A_4 \times \mathbb{Z}_5$, and A_5 , in both in-domain and out-of-distribution settings.

Next, to provide a mechanistic explanation for this success, we apply interpretability techniques to analyze the algorithms learned by Transformer+CoT. Using activation patching (Vig et al., 2020), we identify the circuits (specific model components) responsible for state tracking and observe that Transformer+CoT relies heavily on late-layer MLP neurons. These neurons can be effectively grouped into states based on transition rules. To quantify this, we introduce two metrics: compression and distinction. Compression measures the similarity of representations for the same state under different input prompts, while distinction quan-

tifies the separation between different states, even when their inputs are similar. We find nearly 100% accuracy on both metrics at every intermediate step, providing strong evidence that the model reconstructs the world model (i.e., FSA). For instance, in Figure 1, Transformer+CoT compresses inputs corresponding to two states (i.e. q_0 and q_1) by activating two distinct sets of neurons. Additionally, we observe shifts in attention patterns as the number of intermediate steps increases.

To evaluate robustness in real-world scenarios, we test Transformer+CoT under three challenging settings: skip-step reasoning, noisy scratchpads, and length generalization. Our results show that Transformer+CoT learns robust algorithms even in noisy environments, indicating that the underlying FSA is resilient. This robustness supports the implementation of state tracking in more complex tasks, providing a theoretical foundation for downstream applications.

In summary, this work is the first to extend the study of learnability and expressiveness through mechanistic interpretation, uncovering the underlying algorithms of Transformer+CoT. Our contributions are as follows:

1. We conduct a comprehensive evaluation of the state tracking capabilities of Transformer+CoT, demonstrating its unique ability to track states of arbitrary lengths across multiple groups (\mathbb{Z}_{60} , $A_4 \times \mathbb{Z}_5$, and A_5) in both in-domain and out-of-distribution settings.
2. Using interpretability techniques, including activation patching, we analyze the learned algorithms in Transformer+CoT. We identify the activation of late-layer MLP neurons and classify them into states based on transition rules, achieving nearly 100% accuracy in metrics of compression and distinction, which confirms the model’s reconstruction of the world model (FSA).
3. We explore Transformer+CoT in three challenging settings and find that it learns resilient algorithms capable of effective state tracking in noisy conditions.

2 Related Work

2.1 FSA and State Tracking

We adopt the conventional definition of a finite state automaton (FSA) as a tuple $\mathcal{A} = (\Sigma, Q, q_0, \delta)$, where Σ is the alphabet, Q is a set of states, q_0

²The state tracking problem \mathbb{Z}_2 is equivalent to parity, a formal language describing binary sequences with specific evenness or oddness properties.

is the initial state, and δ is the transition function (Hopcroft and Ullman, 1979). State tracking can be framed as solving a word problem over a finite monoid (M, \cdot) , where the objective is to compute the product $m_1 \cdot m_2 \cdot \dots \cdot m_n \in M$ (Merrill et al., 2024). This computation can be performed by a finite state automaton. As generative models, transformers augmented with chain-of-thought generate state sequences $q_1 \dots q_n \in M^*$ based on input sequences $m_1 \dots m_n \in M^*$. Our work focuses on word problems over groups, specifically the cyclic group \mathbb{Z}_m and the symmetric group S_m .

2.2 Mechanistic Interpretability

The use of mechanistic interpretability (Rai et al., 2024; Ferrando et al., 2024) to explain LLMs is an emerging research direction. This approach employs various techniques, including logit lens (Geva et al., 2021), probing (Gurnee et al., 2023), causal mediation analysis (Wang et al., 2022), sparse autoencoders (Cunningham et al., 2023), and visualization (Cooney and Nanda, 2023), to identify and analyze the features and circuits of LLMs.

3 Evaluating State Tracking Capability Across Architectures

Besides standard transformer and CoT, there are various theoretical works (Zhang et al., 2024; Fan et al., 2024; Yang et al., 2022; Fan et al., 2021) attempting to inject recurrence into transformers, while another line of work (Goyal et al., 2024; Hao et al., 2024) proposing modifications of chain-of-thought (implicit chain-of-thought in contrast to explicit chain-of-thought). In this section, we will explore the state tracking capability with an empirical lens: can standard transformer with/without CoT and these variants successfully learn state tracking?

Dataset: $A_5, A_4 \times \mathbb{Z}_5, \mathbb{Z}_{60}$. Following the formal definition of state tracking in (Merrill et al., 2024; Grazi et al., 2024), we model state tracking as word problems, and consider three kinds of groups with increasing difficulty: \mathbb{Z}_{60} , an abelian group encoding mod-60 addition, $A_4 \times \mathbb{Z}_5$, a non-abelian but solvable group, which is a direct product group of one alternating group A_4 (a subgroup of the symmetric group S_4 containing only even permutations) and one cyclic group \mathbb{Z}_5 , and A_5 , the alternating group on five elements, which is the smallest non-solvable subgroup. With the same number of elements 60, the three groups belong to TC^0 , TC^0 , and NC^1 -complete respectively, with vary-

ing difficulty mainly deriving from the complexity of learning the group multiplication operation.

Architectures. We choose a GPT2-like (Radford et al., 2019) transformer with chain-of-thought (denoted as Transformer+CoT), choose the realistic setting with a bounded number of layers, and log-precision. To compare Transformer+CoT with other models, we also consider recurrent neural networks (RNNs Jain and Medsker, 1999 and LSTMs Hochreiter and Schmidhuber, 1997), S4 (Gu et al., 2022), Mamba (Gu and Dao, 2024), implicit chain-of-thought: transformers with pause (denoted as Pause) (Goyal et al., 2024) and other variants of transformers: standard recurrent transformer (denoted as Recurrent) (Yang et al., 2022), looped transformer (denoted as Looped) (Fan et al., 2024). In order to disentangle recursion introduced by CoT from other variants, we classify different models into encoder and decoder and adopt the Token-Tagging task (TT) and Language Modeling task (LM), respectively. Only Transformer+CoT and implicit CoT (Pause) are designed as decoders, while other models or variants encoder. The reason we design some models as encoders rather than decoders without CoT is that, we use the same labels whether the model is an encoder or decoder, in order to eliminate the influence of labels on supervised training, like the hint setting in (Li et al., 2024). So that we can contribute the performance improvement to recurrence in the structure for variants without chain-of-thought. Model details refer to Appendix B.

Performance (In-Domain). We hold a comprehensive evaluation of models' state tracking capability on word problems, with the same model depth and dimension. We fix the same number of layers and same model dimension for all models of log-precision. We use sequence accuracy as a metric, where the generated sequence is true only when same to ground truth sequence. Figure 2 gives different models' performance across different input sequence length and different groups. We draw several conclusions:

1. Consistent with theoretical study (Liu et al., 2023a; Merrill et al., 2024), transformers and state-space models can not express arbitrary length A_5 word problems, in contrast to RNN and LSTM.
2. $O(N)$ intermediate steps extend the expressive power of transformers. In particular,

Transformer+CoT can empirically converge to a nearly perfect generative model on word problems of arbitrary length, which allows for parallel training and a smoother flow of gradients like Transformer due to no architecture change. However, other variants of transformers (Pause, Looped, and Recurrent) fail to converge on longer sequence lengths, despite postponing the accuracy drop to longer lengths compared to the standard transformer.

3. Expressiveness doesn't equal learnability. Although $A_4 \times \mathbb{Z}_5$ belongs to TC^0 , it can not be learned by models with circuit complexity TC^0 on sequences of arbitrary length.
4. Transformer+CoT achieve a dual win in both expressiveness and learnability. The model not only achieves higher expressiveness than the vanilla transformer but also successfully converges to sequences that are 100 times the number of layers.

Performance (Out-of-Distribution). (Liu et al., 2023a) analyze transformers' failure in out-of-distribution of parity, and argue that transformers learn a shortcut solution, which compute the parity by counting the number of 1s in the input sequences and compute mod-2, thus failing to generalize to sequences with unseen sum of 1s. (Zhang et al., 2024) discuss the role of chain-of-thought in computability, and point that CoT simulates the recurrent connection by iteratively encode and decode back and forth between states and tokens. *The key of Transformer+CoT's expressiveness on state tracking is that previous computation can be retrieved, through concatenating previous step state to the end of scratchpad.*

To investigate whether Transformer+CoT learns an algorithm based solely on the input sequences $m_1 \dots m_n$ or combines input and scratchpad as theoretical work expects, We divide the elements of the three groups into proper subsets. And we train the model on sequences with m belonging to one proper subset, but evaluate on the full set. We stress that, through restricting the input sequences into separate subsets, the possible state sequences remain the same, for the reason that any subset can express the whole group through group operation. If the model learns a shortcut solution, that attends to only input, it can not generalize to sequences with group elements sampled from the full set, because the model has not seen mixed input sequences in the training set. As outlined in Section 3, both

LSTM and Transformer+CoT successfully learn all word problems in-distribution, and we test their performance in out-of-distribution. Results in Figure 2 show that Transformer+CoT achieves perfect generalization on three groups \mathbb{Z}_{60} , $A_4 \times \mathbb{Z}_5$, A_5 in contrast to LSTM, implying that the model attends to not only input but also scratchpad. We provide more experimental settings in Appendix C. The out-of-distribution performance eliminates the possibility that the model learns specific shortcuts similar to those Liu et al. (2023a) found on \mathbb{Z}_2 group, but this does not rule out the possibility that other shortcuts exist, which necessitates an interpretation on the mechanism.

4 Mechanism Inside Transformer+CoT: FSA

Both transformers with chain-of-thought and recurrent neural network achieve perfect performance within distribution, and the former even generalize well in out-of-distribution. Due to the transformer's black-box nature, the mechanism behind its implementation of state tracking remains unknown, and we cannot answer the questions that what algorithm the model has learned to keep track of world state, and to what extent the model can generalize. Considering that the word problems involves a series of state transitions, the model's state computation is dynamic and consecutive while generating intermediate steps. In this section, we try to analyze the circuit transformers with chain-of-thought use to keep track of world state first, and then hold deep component analysis to interpret the mechanism.

4.1 Circuit Localization

To understand the mechanism of state tracking, we will first localize the circuit (a subset of components) using activation patching (Vig et al., 2020). We format the word problems as prompt $p_i = m_1 \dots m_n | q_i \dots q_{i-1}$ and result state token q_i at i -th step. At each intermediate step, we sample a prompt p_i with its corresponding result state q_i , and then sample a counterfactual prompt p'_i , resulting in a different result state q'_i . We hold intervention experiments, by replacing the activation of a specific MLP layer or attention head with the pre-computed for p'_i , and then assessing how this impacts the probabilities of answer tokens. To access the importance of one component at i -th step, we average the following intervention effect (IE) metric (Nikankin et al., 2024) across all prompts,

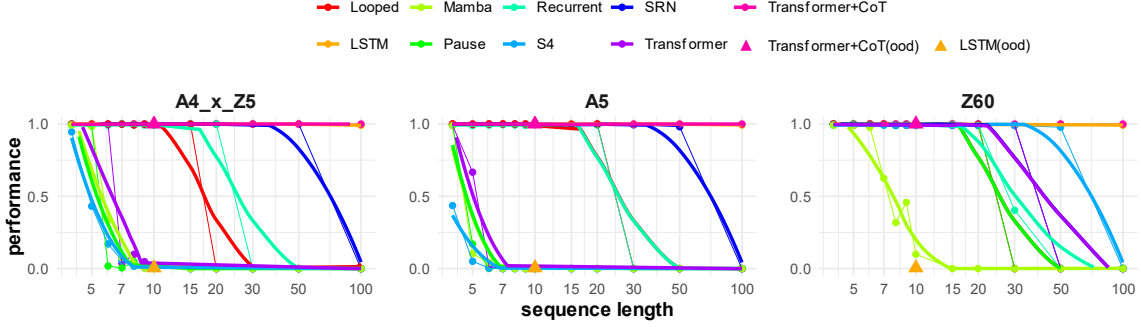


Figure 2: Model accuracy across sequence lengths for Z_{60} , $A_4 \times Z_5$ and A_5 .

which is the mean of impacts of q_i and q'_i :

$$\mathbb{E}(q_i, q'_i) = \frac{1}{2} \left[\frac{P^*(q'_i) - P(q'_i)}{P(q'_i)} + \frac{P(q_i) - P^*(q_i)}{P^*(q_i)} \right]$$

where P and P^* are the pre- and post-intervention probability distributions.

We localize the circuit Transformer+CoT use to keep track of world state at each intermediate step in A_5 word problems. As Figure 3 shows, we find that the circuit across each intermediate step mainly consists of MLPs, with attention heads few impacts. And across each intermediate step, the circuit has hardly changed, that is, the first MLP (MLP0 [McDougall et al., 2023](#)) in position m_i and late-layer MLPs in last position play a significant role in state tracking at the i -th step. Above all, given input sequences $m_1 \dots m_n \in M^*$ concatenated with scratchpad $q_1 \dots q_{i-1} \in M^*$, the MLPs mainly implement state transition, and the late-layer MLPs in the last position q_{i-1} promote the correct token q_i .



Figure 3: Activation patching results for A_5 word problems of length 10 at 4-th step, with the prompt $p_5 = m_1 \dots m_{10} | q_1 \dots q_4$ and ground truth q_5 .

4.2 MLP Neuron Analysis

Having identified the circuit, we then hold deeper component analysis on how late-layer MLPs implement state tracking. [Geva et al. \(2022\)](#) point

out that the MLP contributes additive updates to the residual stream, which can be further decomposed into weighted collections of sub-updates. In particular, given input x^l at layer l , MLP can be expressed using the parameters $K^l, V^l \in \mathbb{R}^{d_{mlp} \times d_m}$, where d_{mlp} is the MLP intermediate dimension and d_m is the model dimension. Additionally, a non-linear activation function f is applied:

$$MLP^l(x^l) = f(K^l x^l) V^l$$

Expanding this further, it can be decomposed as:

$$MLP^l(x^l) = \sum_{j=1}^{d_{mlp}} f(x^l \cdot k_j^l) v_j^l = \sum_{j=1}^{d_{mlp}} m_j^l v_j^l$$

where $k_j^l \in \mathbb{R}^d$ and $v_j^l \in \mathbb{R}^d$ correspond to the j -th row vectors of K^l and V^l , respectively. The scalar $m_j^l = f(x^l \cdot k_j^l)$ represents the activation coefficient associated with the neuron v_j^l . Notably, when mapped into the vocabulary space, these individual sub-updates $m_j^l v_j^l$ can be interpreted in a human-understandable manner ([Geva et al., 2022](#)).

We first group all possible prompts into prompt subsets according to the resulting world state. Specifically, any prompt $m_1 \dots m_n | q_i \dots q_{i-1}$ at i -th step in one subset should reduce to the same state q_i under group operation (for simplicity, denoted as \mathbf{q} prompt subset³). On each \mathbf{q} prompt subset, we calculate the contribution of each late-layer MLP to \mathbf{q} in the layer representation using logit lens ([Geva et al., 2021](#)) and average on all intermediate steps. The results in Figure 4 show that, among late-layer MLPs, the last three layers of MLP play a significant role and MLP11 mainly implements the state transition, accounting for the 72% logit increase.

³We use \mathbf{q} to represent q_i

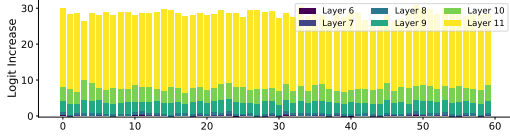


Figure 4: Average state \mathbf{q} logit increase in the layer representation for different late-layer MLPs.

To analyze what the MLP neurons’ activation pattern is, we divide the prompts into different (m_i, q_{i-1}) pairs (for simplicity, (m, q) pairs⁴), where m_i is the i -th input element, and q_{i-1} is the previous world state. We analyze the activation pattern of MLP neurons in layer l across all (m, q) pairs. Interestingly, late-layer MLP neurons get activated only on a specific subset of all (m, q) pairs (denoted as *predictions*). More specifically, the top 60 (m, q) pairs are distributed across each row or column. Interestingly, according to the transition rules, there are 60 (m, q) pairs deducing to state \mathbf{q} (corresponding to \mathbf{q} prompt subset), distributed across each row and column (denoted labels). Based on this, we can ask the following questions:

- Q1: Does the activation pattern correspond to a bag of MLP neurons being activated on the \mathbf{q} prompt subset, which deduces to state \mathbf{q} according to transition rules?
- Q2: Can we classify the MLP neurons according to the resulting states?

To answer the questions, we hold neurons classification experiments (with the detailed procedures provided in Appendix D) to classify all MLP neurons at layer l . Through this experiment, we successfully mapped the MLP11, MLP10 and MLP9 neurons to states with successful ratio 90.0%, 79.6% and 38.7%. Furthermore, nearly 15.5% MLP11 neurons even have perfect f1 score with the ground truth subset of (m, q) pairs, meaning the neuron to state mapping N to 1. After classifying neurons into states, we can compute the accuracy and recall of the activated neurons, refer to Appendix F for details.

For Q1, most neurons have high f1 score with ground truth subset of (m, q) pairs of state \mathbf{q} , which means that the neurons get activated on \mathbf{q} prompt subset, which deduce to state \mathbf{q} according to transition rules. For Q2, we can classify all activated

⁴We use q to represent q_{i-1} .

neurons at layer l across intermediate steps, and even 15.5% MLP11 neurons satisfy N to 1 mapping. We can conclude that transformers with chain-of-thought keep track of world state through a bag of late-layer MLP neurons, which get activated in specific subset of (m, q) pairs, and promote correct state token \mathbf{q} to the residual stream. Moreover, a correct state transition is achieved through the collective sub-updates of multiple neurons, that belong to the state \mathbf{q} . Beyond the late-layer MLPs, we also analyze another significant component of the circuit, MLP0, which primarily achieves effective embedding of m_i for subsequent state transitions. Further details can be found in Appendix G.

4.3 Transformer+CoT Recovers FSA

Nearly perfect in next-token prediction does not necessarily imply that the generative model has reconstructed the world model to the same extent, for example, cumulative Connect-4 in (Vafa et al., 2024). In terms of state tracking, the world model FSA can compress different sequences as long as they deduce to the same state, and distinguish sequences as long as they deduce to different states, no matter how similar the sequences are. As a generative model, Transformer+CoT has achieved nearly perfect sequence accuracy in word problems, while the learned structure remains under-researched. Results in Section 4.2 imply that the model implements state tracking, through activating a bag of neurons. Based on this, we can measure the generative model’s FSA recovery, from the perspective of sequence compression and distinction at the granularity of the MLP neurons. For activated neurons on two prompts p_i, p'_i deducing to the same state, we design the following compression metric:

$$\text{Compression} = \frac{|N_{p_i} \cap N_{p'_i}|}{|N_{p_i} \cup N_{p'_i}|}$$

where $N_{p_i}, N_{p'_i}$ represent activated neurons on p_i, p'_i . And for activated neurons on two prompts p_i, p'_i deducing to different states, we design the following distinction metric:

$$\text{Distinction} = 1 - \frac{|N_{p_i} \cap N_{p'_i}|}{|N_{p_i} \cup N_{p'_i}|}$$

For each intermediate step, we calculate compression and distinction pairwise in all m, q pairs. We find that Transformer+CoT can not only compress prompts sampled from the \mathbf{q} prompt subset, but also

distinguish prompts from different subsets with average metric close to 1, at each intermediate step. Beyond A_5 , we also find the similar FSA existing on \mathbb{Z}_{60} and $A_4 \times \mathbb{Z}_5$, and large model scales, with details referring to Appendix H. And we conclude that *Transformer+CoT recovers FSA on state tracking even at the granularity of MLP neurons*.

4.4 Dynamic Circuit Analysis: Attention Patterns

In the context of state tracking, the model’s circuit is dynamic and consecutive during inferring each state q_i in the scratchpad. Previous sections mainly analyze the MLP circuit as static circuit composed of late-layer MLPs, in this section we focus on the dynamic attention patterns across intermediate steps. We first obtain the principal attention heads based on the activation patching results in Section 4.1 and analyze their activation patterns. Results in Figure 5 show that there are two kinds of attention patterns:

1. Across all steps, specific attention heads transfer information from position m_i to position q_{i-1} .
2. As the sequence length increases, the model has developed another attention pattern: the model passes the information from $m_1 \dots m_n$ backwards until the delay position “:”, which splits input and scratchpad and marks the beginning of state tracking, so that the model can attend to the delay position during inference.

We discuss more about the two attention patterns in Appendix I.

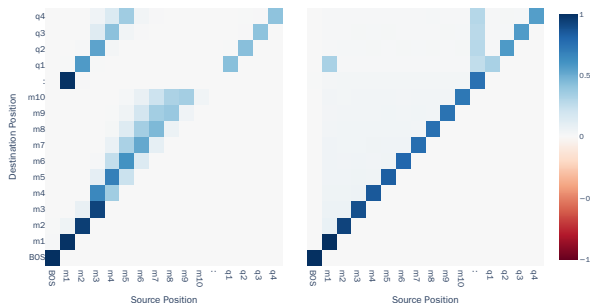


Figure 5: Two attention patterns.

5 Robustness and Generalizability of FSA

Sections 3 and 4 have demonstrated positive results in FSA recovery. However, the word problems

considered are too idealistic, with sequence length controlled and noise excluded. And the actual data distribution may differ from this. In this section, we will investigate the robustness and generalizability of FSA inside Transformer+CoT, considering intermediate step jumps, scratchpad noise, and length generalization. We found that optimizing the distribution of training set data can guide the learned model to adapt to the above scenarios, except for length generalization. And solving the latter may necessitate exploring different perspectives, such as modifying the model architecture, improving training strategies, or other.

5.1 Allow Skipping

In practical training data, intermediate step jumps are very common. For example, the length of $q_1 \dots q_n$ may be less than n , with some intermediate steps skipped. In our experiment setting, we skip each intermediate state q_i except q_n with skipping probability, and train Transformer+CoT in the dataset. In order to study the extent of the model’s step jumps, we use a linear classifier to probe the states embedded in the residual stream in the last position. Specifically, we probe the token q_i in the last position, given the prompt $m_1 \dots m_n | q_1 \dots q_{i-1}$. From the results in Figure 6, we can find that q_i , q_{i+1} , and q_{i+2} are all embedded in the residual stream, suggesting that the model has learned single-step reasoning, two-step reasoning (skipping one step), as well as three-step reasoning (skipping two steps). Moreover, we find that the index of layers with sufficiently high probing results for q_{i+2} is greater than that for q_{i+1} , which is greater than that for q_i in turn. Moreover, we propose possible mechanisms for skipping and design experiments for analysis as in the appendix J. Finally, we conclude that adding skipping to the training set can guide the FSA inside Transformer+CoT to adapt to the scenario.

5.2 Noise in Scratchpad

In this section, we consider injecting noise into scratchpad $q_1 \dots q_{i_1}$, where some previous state is false. We divide the noise into the following two types: any false state except q_{i-1} and false q_{i-1} . We have tested the accuracy of the model in predicting the next token with noise in scratchpad (we use token accuracy as metric here). For the first type noise, the model still achieves almost perfect predictions. The reason is obvious: when the model implements state transition in the i -th

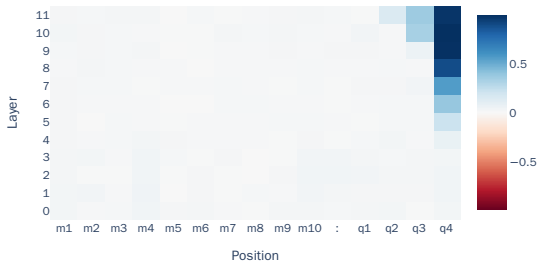


Figure 6: Probing results for state q_i at 4-th step. We can find the positive results appearing two positions earlier.

step, it mainly focuses on m_i and the previous state q_{i-1} , while ignoring intermediate states prior to q_{i-1} . And for the second type of noise, the model’s performance dramatically decreases to an average accuracy of nearly zero (0.017).

Here, we attempt once again to deal with the scenario by adjusting the dataset distribution. Specifically, we train the model using the data with the second type of noise in scratchpad and successfully enhanced the robustness of the model, with the second type noise accuracy increased from 0.017 to 0.896. Furthermore, we probe the layer representation in the last position to investigate whether the model has retrieved correct state tracking. Specifically, given the corrupt prompt $m_1 \dots m_n | q_1 \dots q_{i-1}$ (q_{i-1} stands for the error state), we probe the correct next state q_i , false previous state q_{i-1} and true previous state q_{i-1} . We find that the layer representation maintains positive probing results for q_{i-1} until the MLP11, which exhibits high accuracy for q_i , and low for q_{i-1} . Based on this, we propose one possible mechanism that the model attends to intermediate representation at previous step, thus retrieving the correct input state q_{i-1} and updating the state to q_i successfully. And we have designed experiments to analyze the hypothesis as in Appendix K. We conclude that optimizing dataset distribution can help in maintaining the accuracy and reliability of the FSA inside Transformer+CoT.

5.3 Length Generalization and Error Analysis

Furthermore, we investigate length generalization in out-of-distribution setting, which is a critical challenge in the development of transformer-based language models. We replace GPT2’s original absolute positional embedding with NoPE (without ex-

PLICIT positional embedding) for better length generalization performance, which has been proven to resemble T5’s relative positional embedding (Kazemnejad et al., 2024). And we choose LSTM for comparison for the reason that it learns any word problems on sequences of arbitrary length. Table 1 shows that on sequences of lengths that it has not ever seen during training, different models exhibit varying levels of length generalization ability: LSTM perfect, while transformers with chain-of-thought weak. We analyze the failure from the perspective of MLP neurons, and find an interesting “U-turn” phenomenon in activated neurons precision during the last few steps of inference. More analysis on this phenomenon refers to the Appendix L. Finally, we conclude that improving the length generalization ability of the model requires other methods, perhaps the model structure, loss function or optimization algorithm.

Models	20	21	22	23	24	25	30
LSTM	1	1	1	1	1	1	1
Transformer+CoT	0.99	0.983	0.868	0.527	0.24	0.088	0

Table 1: Length generalization performance of LSTM and Transformer+CoT. The models are trained on sequences of length up to 20.

6 Conclusions

In this work, we investigate the learnability of Transformer+CoT through the lens of mechanistic interpretability in state tracking. We begin by reaffirming the success of Transformer+CoT in both in-domain and out-of-domain settings. Next, we identify the key components of the circuit, specifically the neurons in the last layers of the MLP, which play a critical role. We find evidence of an implicit FSA within the model, where each state is compressed by a distinct set of neurons. Finally, we evaluate the model in three realistic settings and show that the learned FSA is robust to noise and sequence skipping but struggles with generalization to significantly longer sequences. This suggests the need for architectural or optimization improvements. Our findings reveal that Transformer+CoT achieves near-perfect performance in next-token prediction while internalizing an FSA-like structured state representation, bridging the gap between expressiveness and learnability. This work provides insights into structured reasoning for sequential tasks.

Limitations

In this paper, we define state tracking as word problems involving cyclic and symmetric groups, which form the basis of our conclusions. Our study focuses solely on GPT2-like models, leaving the exploration of additional models, such as Llama, for future research. Furthermore, while we have made efforts to address more realistic word problems, state tracking in real-world tasks is intricate, making it challenging to separate state tracing abilities from other skills.

References

- Satwik Bhattamishra, Kabir Ahuja, and Navin Goyal. 2020. *On the Ability and Limitations of Transformers to Recognize Formal Languages*. In *Proceedings of the 2020 Conference on Empirical Methods in Natural Language Processing (EMNLP)*, pages 7096–7116, Online. Association for Computational Linguistics.
- Alan Cooney and Neel Nanda. 2023. *Circuitsvis*. <https://github.com/TransformerLensOrg/CircuitsVis>.
- Hoagy Cunningham, Aidan Ewart, Logan Riggs, Robert Huben, and Lee Sharkey. 2023. *Sparse autoencoders find highly interpretable features in language models*. *Preprint*, arXiv:2309.08600.
- Grégoire Delétang, Anian Ruoss, Jordi Grau-Moya, Tim Genewein, Li Kevin Wenliang, Elliot Catt, Chris Cundy, Marcus Hutter, Shane Legg, Joel Veness, and Pedro A. Ortega. 2023. *Neural networks and the chomsky hierarchy*. *Preprint*, arXiv:2207.02098.
- Angela Fan, Thibaut Lavril, Edouard Grave, Armand Joulin, and Sainbayar Sukhbaatar. 2021. *Addressing some limitations of transformers with feedback memory*. *Preprint*, arXiv:2002.09402.
- Ying Fan, Yilun Du, Kannan Ramchandran, and Kangwook Lee. 2024. *Looped transformers for length generalization*. *Preprint*, arXiv:2409.15647.
- Javier Ferrando, Gabriele Sarti, Arianna Bisazza, and Marta R. Costa-jussà. 2024. *A primer on the inner workings of transformer-based language models*. *Preprint*, arXiv:2405.00208.
- Mor Geva, Avi Caciularu, Kevin Wang, and Yoav Goldberg. 2022. *Transformer feed-forward layers build predictions by promoting concepts in the vocabulary space*. In *Proceedings of the 2022 Conference on Empirical Methods in Natural Language Processing*, pages 30–45, Abu Dhabi, United Arab Emirates. Association for Computational Linguistics.
- Mor Geva, Roei Schuster, Jonathan Berant, and Omer Levy. 2021. *Transformer feed-forward layers are key-value memories*. *Preprint*, arXiv:2012.14913.
- Sachin Goyal, Ziwei Ji, Ankit Singh Rawat, Aditya Krishna Menon, Sanjiv Kumar, and Vaishnavh Nagarajan. 2024. *Think before you speak: Training language models with pause tokens*. *Preprint*, arXiv:2310.02226.
- Riccardo Grazi, Julien Siems, Jörg K. H. Franke, Arber Zela, Frank Hutter, and Massimiliano Pontil. 2024. *Unlocking state-tracking in linear rnns through negative eigenvalues*. *Preprint*, arXiv:2411.12537.
- Albert Gu and Tri Dao. 2024. *Mamba: Linear-time sequence modeling with selective state spaces*. *Preprint*, arXiv:2312.00752.
- Albert Gu, Karan Goel, and Christopher Ré. 2022. *Efficiently modeling long sequences with structured state spaces*. *Preprint*, arXiv:2111.00396.
- Wes Gurnee, Neel Nanda, Matthew Pauly, Katherine Harvey, Dmitrii Troitskii, and Dimitris Bertsimas. 2023. *Finding neurons in a haystack: Case studies with sparse probing*. *Preprint*, arXiv:2305.01610.
- Simeng Han, Hailey Schoelkopf, Yilun Zhao, Zhenyuan Qi, Martin Riddell, Wenfei Zhou, James Coady, David Peng, Yujie Qiao, Luke Benson, Lucy Sun, Alex Wardle-Solano, Hannah Szabo, Ekaterina Zubova, Matthew Burtell, Jonathan Fan, Yixin Liu, Brian Wong, Malcolm Sailor, Ansong Ni, Linyong Nan, Jungo Kasai, Tao Yu, Rui Zhang, Alexander R. Fabbri, Wojciech Kryscinski, Semih Yavuz, Ye Liu, Xi Victoria Lin, Shafiq Joty, Yingbo Zhou, Caiming Xiong, Rex Ying, Arman Cohan, and Dragomir Radev. 2024. *Folio: Natural language reasoning with first-order logic*. *Preprint*, arXiv:2209.00840.
- Shibo Hao, Sainbayar Sukhbaatar, DiJia Su, Xian Li, Zhiting Hu, Jason Weston, and Yuandong Tian. 2024. *Training large language models to reason in a continuous latent space*. *Preprint*, arXiv:2412.06769.
- Sepp Hochreiter and Jürgen Schmidhuber. 1997. *Long short-term memory*. *Neural Computation*, 9(8):1735–1780.
- J. E. Hopcroft and J. D. Ullman. 1979. *Introduction to Automata Theory, Languages, and Computation*. Addison-Wesley, Reading, MA.
- L. C. Jain and L. R. Medsker. 1999. *Recurrent Neural Networks: Design and Applications*, 1st edition. CRC Press, Inc., USA.
- Amirhossein Kazemnejad, Inkit Padhi, Karthikeyan Natesan Ramamurthy, Payel Das, and Siva Reddy. 2024. *The impact of positional encoding on length generalization in transformers*. In *Proceedings of the 37th International Conference on Neural Information Processing Systems, NIPS '23*, Red Hook, NY, USA. Curran Associates Inc.
- Najoung Kim and Sebastian Schuster. 2023. *Entity tracking in language models*. In *Proceedings of the 61st Annual Meeting of the Association for Computational Linguistics (Volume 1: Long Papers)*, pages

- 3835–3855, Toronto, Canada. Association for Computational Linguistics.
- Zhiyuan Li, Hong Liu, Denny Zhou, and Tengyu Ma. 2024. [Chain of thought empowers transformers to solve inherently serial problems](#). *Preprint*, arXiv:2402.12875.
- Bingbin Liu, Jordan T. Ash, Surbhi Goel, Akshay Krishnamurthy, and Cyril Zhang. 2023a. [Transformers learn shortcuts to automata](#). *Preprint*, arXiv:2210.10749.
- Xiao Liu, Hao Yu, Hanchen Zhang, Yifan Xu, Xunyu Lei, Hanyu Lai, Yu Gu, Hangliang Ding, Kaiwen Men, Kejuan Yang, Shudan Zhang, Xiang Deng, Aohan Zeng, Zhengxiao Du, Chenhui Zhang, Sheng Shen, Tianjun Zhang, Yu Su, Huan Sun, Minlie Huang, Yuxiao Dong, and Jie Tang. 2023b. [Agentbench: Evaluating llms as agents](#). *Preprint*, arXiv:2308.03688.
- Callum McDougall, Arthur Conmy, Cody Rushing, Thomas McGrath, and Neel Nanda. 2023. [Copy suppression: Comprehensively understanding an attention head](#). *Preprint*, arXiv:2310.04625.
- William Merrill, Jackson Petty, and Ashish Sabharwal. 2024. [The illusion of state in state-space models](#). *Preprint*, arXiv:2404.08819.
- Merrill, William and Sabharwal, Ashish. 2024. A logic for expressing log-precision transformers. In *Proceedings of the 37th International Conference on Neural Information Processing Systems, NIPS '23*, Red Hook, NY, USA. Curran Associates Inc.
- Yaniv Nikankin, Anja Reusch, Aaron Mueller, and Yonatan Belinkov. 2024. [Arithmetic without algorithms: Language models solve math with a bag of heuristics](#). *Preprint*, arXiv:2410.21272.
- Maxwell Nye, Anders Johan Andreassen, Guy Gur-Ari, Henryk Michalewski, Jacob Austin, David Bieber, David Dohan, Aitor Lewkowycz, Maarten Bosma, David Luan, Charles Sutton, and Augustus Odena. 2021. [Show your work: Scratchpads for intermediate computation with language models](#). *Preprint*, arXiv:2112.00114.
- OpenAI. 2023. [Gpt-4 technical report](#). *arXiv preprint arXiv:2303.08774*.
- Ruizhong Qiu, Zhe Xu, Wenxuan Bao, and Hanghang Tong. 2024. [Ask, and it shall be given: Turing completeness of prompting](#). *Preprint*, arXiv:2411.01992.
- Alec Radford, Jeffrey Wu, Rewon Child, David Luan, Dario Amodei, Ilya Sutskever, et al. 2019. Language models are unsupervised multitask learners. *OpenAI blog*, 1(8):9.
- Daking Rai, Yilun Zhou, Shi Feng, Abulhair Saparov, and Ziyu Yao. 2024. [A practical review of mechanistic interpretability for transformer-based language models](#). *Preprint*, arXiv:2407.02646.
- Shubham Toshniwal, Sam Wiseman, Karen Livescu, and Kevin Gimpel. 2022. [Chess as a testbed for language model state tracking](#). *Preprint*, arXiv:2102.13249.
- Hugo Touvron, Thibaut Lavril, Gautier Izacard, Xavier Martinet, Marie-Anne Lachaux, Timothée Lacroix, Baptiste Rozière, Naman Goyal, Eric Hambro, Faisal Azhar, Aurelien Rodriguez, Armand Joulin, Edouard Grave, and Guillaume Lample. 2023. [Llama: Open and efficient foundation language models](#). *Preprint*, arXiv:2302.13971.
- Keyon Vafa, Justin Y. Chen, Ashesh Rambachan, Jon Kleinberg, and Sendhil Mullainathan. 2024. [Evaluating the world model implicit in a generative model](#). *Preprint*, arXiv:2406.03689.
- Karthik Valmeekam, Kaya Stechly, and Subbarao Kambhampati. 2024. [Llms still can't plan; can llms? a preliminary evaluation of openai's o1 on planbench](#). *Preprint*, arXiv:2409.13373.
- Jesse Vig, Sebastian Gehrmann, Yonatan Belinkov, Sharon Qian, Daniel Nevo, Yaron Singer, and Stuart Shieber. 2020. Investigating gender bias in language models using causal mediation analysis. In *Proceedings of the 34th International Conference on Neural Information Processing Systems, NIPS '20*, Red Hook, NY, USA. Curran Associates Inc.
- Kevin Wang, Alexandre Variengien, Arthur Conmy, Buck Shlegeris, and Jacob Steinhardt. 2022. [Interpretability in the wild: a circuit for indirect object identification in gpt-2 small](#). *Preprint*, arXiv:2211.00593.
- Jason Wei, Xuezhi Wang, Dale Schuurmans, Maarten Bosma, Brian Ichter, Fei Xia, Ed Chi, Quoc Le, and Denny Zhou. 2023. [Chain-of-thought prompting elicits reasoning in large language models](#). *Preprint*, arXiv:2201.11903.
- Jiewen Yang, Xingbo Dong, Liujun Liu, Chao Zhang, Jiajun Shen, and Dahai Yu. 2022. [Recurring the transformer for video action recognition](#). In *2022 IEEE/CVF Conference on Computer Vision and Pattern Recognition (CVPR)*, pages 14043–14053.
- Xiang Zhang, Muhammad Abdul-Mageed, and Laks V. S. Lakshmanan. 2024. [Autoregressive + chain of thought = recurrent: Recurrence's role in language models' computability and a revisit of recurrent transformer](#). *Preprint*, arXiv:2409.09239.
- Hattie Zhou, Arwen Bradley, Etai Littwin, Noam Razin, Omid Saremi, Josh Susskind, Samy Bengio, and Preetum Nakkiran. 2023. [What algorithms can transformers learn? a study in length generalization](#). *Preprint*, arXiv:2310.16028.

A Symbol Description

In this section, we briefly introduce the symbols used in this article as in Table 2.

B Model used for Performance Evaluation

In Section 3, we hold a comprehensive evaluation on various model variants and implicit CoT. The models and task designs are listed as Table 3.

C Separating Elements in Groups

In Section 3, we separate all m into proper subsets to explore the models' performance. As Table 4 shows, we divide m in \mathbb{Z}_{60} , $A4_x_Z5$ and A_5 according to values, orders and permutation types, respectively. We then prove that the division is reasonable, for the reason that every proper subset can generate the whole group.

Theorem 1 *Every separated proper subset can generate the whole group under group operation.*

Proof C.1 *For Cyclic group, every element is a generator; so that proper subsets can generate $h \in \mathbb{Z}_{60}$.*

For alternating group, the 3-cycle and 5-cycle in A_5 can both generate the group.

For direct product group, we continue the proof as follows:

The elements of order 15 in the direct product group $A_4 \times \mathbb{Z}_5$ are those elements of the form (g, h) , where $g \in A_4$ is a 3-cycle (order 3) and $h \in \mathbb{Z}_5$ is a nonzero element (order 5). Although these elements of order 15 form a proper subset of the entire group, their projections onto the factors A_4 and \mathbb{Z}_5 separately generate the full groups:

- *The 3-cycle in A_4 can generate A_4 (since A_4 is generated by its 3-cycles).*
- *Any nonzero element in \mathbb{Z}_5 is a generator, thus can generate the entire \mathbb{Z}_5 .*

By the generation theorem of direct product groups, if a subset has surjective projections onto each factor, then the group it generates must be the entire direct product. Thus, all elements of order 15 can generate the entire group $A_4 \times \mathbb{Z}_5$.

We train the model with sequences sampled from one subset, and evaluate on sequences with m sampled from the group. We emphasize that Although the model did not encounter mixed sequences during training, the proper subset is able to generate the entire group. Therefore, all possible state transitions are included in the data. Transformer+CoT success in out-of-distribution shows

that the learned algorithm does not rely on finding a certain pattern in the input sequence.

Surprisingly, LSTM fails to generalize when used as an encoder. We have also explored its performance as a decoder, but here, LSTM even fails to converge. We hypothesize that the disparity in out-of-distribution performance stems from LSTM being used as an encoder, whereas Transformer+CoT, as a decoder, can integrate all elements of the group into the sequence by concatenating each possible state after the input sequence.

D Classification Algorithms

We provide the late-layer MLP neurons classification procedures and pseudocode Algorithm 1 as follows:

1. Utilize the priori transition rules to pre-compute all labels across all possible resulting states.
2. Measure all activation coefficient m_j^l across all (m, q) pairs.
3. Utilize the logit lens to calculate the logits of tokens embedded in v_j^l , and convert to a 2D pattern, where the cell in index (m, q) is the logit of the result state $\mathbf{q} = m \cdot q$.
4. Multiply the intermediate results of the previous two steps element-wise, resulting in effective logit contribution of the neuron to the corresponding state for each (m, q) pair.
5. Extract the top 60 (m, q) pairs from the activation pattern as the prediction.
6. Compute the f1 scores between prediction and all labels. The neuron can be classified to state with f1 score no less than threshold $\theta = 0.2^5$.

E Expected F1 Score of Randomly Activated Neurons

In Section 4.2, we empirically set the value of θ as 0.2 to classify MLP neurons, which is non-trivial compared with random F1 score 0.017. And we provide detailed calculation process of randomly activated neurons' F1 score as follows.

Let S be a set containing 3600 elements: $S = \{0, 1, 2, \dots, 3599\}$, and let L be the label set consisting of the first 60 elements: $L = \{0, 1, 2, \dots, 59\}$. We randomly sample 60 elements from S to form a subset x : $x \subseteq S$ and

⁵Here the value of θ is an empirical setting, and the random value is 0.017, refer to Appendix E for the computation of the random value.

Algorithm 1 Classify MLP Neurons at Layer l

- 1: **Input:** Prior transition rules T , activation coefficients matrix M_j^l for all (m, q) pairs, value vector v_j^l , threshold θ
 - 2: **Output:** Classified neurons
 - 3: Compute all labels L from T
 - 4: **for** each neuron j in layer l **do**
 - 5: Compute logit matrix Z_j for all (m, q) pairs from v_j^l using logit lens
 - 6: Compute effective logit contribution $C_j = M_j^l \odot Z_j$
 - 7: Select top 60 (m, q) pairs from C_j as prediction P_j
 - 8: Compute F1 score between P_j and L
 - 9: **if** F1 score $\geq \theta$ **then**
 - 10: Classify neuron j as relevant
 - 11: **else**
 - 12: Classify neuron j as irrelevant
 - 13: **end if**
 - 14: **end for**
 - 15: **return** Classified neurons
-

$|x| = 60$. Our goal is to compute the expected values of precision, recall, and F1 score for the subset x with respect to the label set L .

Define $T = |x \cap L|$ as the number of correctly selected elements. Since x is chosen uniformly at random from S , and given that L contains 60 elements, T follows a hypergeometric distribution. Its expected value is:

$$\mathbb{E}[T] = \frac{|x| \cdot |L|}{|S|} = \frac{60 \times 60}{3600} = 1.$$

The precision and recall are defined by

$$\text{Precision} = \frac{|x \cap L|}{|x|} = \frac{T}{60}$$

$$\text{Recall} = \frac{|x \cap L|}{|L|} = \frac{T}{60}$$

Thus, their expected values are

$$\mathbb{E}[\text{Precision}] = \mathbb{E}\left[\frac{T}{60}\right] = \frac{\mathbb{E}[T]}{60} = \frac{1}{60},$$

$$\mathbb{E}[\text{Recall}] = \frac{1}{60}.$$

The F1 score is the harmonic mean of precision and recall:

$$\text{F1} = \frac{2 \cdot \text{Precision} \cdot \text{Recall}}{\text{Precision} + \text{Recall}}.$$

Since Precision = Recall = $\frac{T}{60}$, we substitute to obtain

$$\text{F1} = \frac{2 \cdot \frac{T}{60} \cdot \frac{T}{60}}{\frac{T}{60} + \frac{T}{60}} = \frac{2 \cdot \frac{T^2}{3600}}{\frac{2T}{60}} = \frac{T}{60}.$$

Hence, the expected F1 score is

$$\mathbb{E}[\text{F1}] = \mathbb{E}\left[\frac{T}{60}\right] = \frac{1}{60} \approx 0.01667.$$

F Activated Neurons Analysis

Having classified neurons into states as in Section 4.2, We can compute the accuracy and recall of the activated neurons, averaged over all \mathbf{q} prompt subsets, during the single-step state transition of the model. We acquire the top- K activated neurons according to the activation coefficient m_j^l , and compute the precision and recall with classified neurons as labels. Results in Figure 7 show that across intermediate steps, the model successfully activate MLP11 neurons with high precision 0.797 but low recall 0.253. We stress that the high precision explains the accuracy on word problems. The low recall imply that, the neurons activated at different steps are also distinguished.

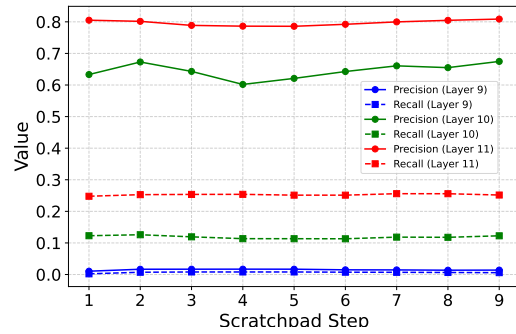


Figure 7: Averaged precision and recall across different steps.

G MLP0 in Circuit

Activation patching results in Section 4.1 show that the circuit mainly consists of MLP0 and late-layer MLPs. Given a prompt $m_1 \dots m_n | q_1 \dots q_{i-1}$, the late-layer MLPs implement state transition in the position q_{i-1} , while the MLP0 mainly achieves effective word embedding in position m_i . As Figure 8 shows, the MLP0 promotes input m_i into the residual stream, which will then be transferred to the last position q_{i-1} by attention heads for subsequent state transitions.

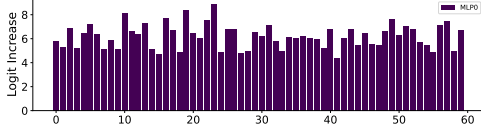


Figure 8: Average input m logit increase in the layer representation for MLP0. The MLP0 mainly implements effective word embedding in the circuit.

H Automata still exists on other groups with large model scale.

We have found FSA with GPT2-small on A_5 as in Section 4.3, in this section, we will extrapolate this conclusion to other problems and models. We first conduct similar experiments on $A_4 \times \mathbb{Z}_5$ and \mathbb{Z}_{60} . We find that MLP11 neurons can still be classified according to transition rules, and the model can still compress and distinguish different input sequences. Moreover, we explore whether FSA still exists with model scale larger. We have repeated the experiments, increasing the model scale from GPT2 small (124M) to GPT2 large (744M), and found FSA still exists. Results are shown in Figure 9.

I Dynamic Attention Pattern

In terms of the attention patterns in Section 4.4, a natural question is how the attention heads extract m_i from the numerous input $m_1 \dots m_n$ embedded in the residual stream at the delay position.

We hypothesize that this extraction depends on the first type of attention pattern, which has injected the input information m_i into the current position, facilitating the second type attention heads to differentiate the mixed information embedded in delay position. Furthermore, we validate this hypothesis by masking position m_i at the q_{i-1} position and probing the changes of retrieving input m_i at the current step. When there is no mask, the average accuracy of probing m_i in the representation of the middle and later layers, except for the last layer (high results for q_i), is greater than 0.9. However, when the mask is applied, it drops to nearly 0. We conclude that, the model uses two interrelated dynamic attention patterns to focus on the correct input m_i at i -th step, corresponding to the FSA accepting each step of the input.

J Allow Skipping

According to the probing results in Figure 6, we propose two possible mechanisms for skipping in

Transformer+CoT: one is to use continuous layers to achieve multi-step state transitions, and the other is to use a single layer to achieve multi-step transitions. The key difference is that the former depends on the skipped states, while the latter does not. To explore what algorithms the model uses in skipping, we design intervention experiments by suppressing skipped tokens. Specifically, given the prompt $m_1 \dots m_n | q_1 \dots q_{i-1}$, we evaluate the probing changes for q_{i+1} in the last position, while suppressing token q_i . We find that suppressing q_i has caused the positive probing results to drop almost to zero in the last position with skipping probability ranging between 0 and 1, suggesting that Transformer+CoT implements skipping through continuous layers.

K Noise in Scratchpad

Based on the probing results in Section 5.2, we propose that at the i -th step, the model mitigates the influence of the incorrect input state q_{i-1} in the final layer while focusing on the intermediate representation from the previous step. This allows it to recover the correct input state q_{i-1} and accurately update to q_i .

To verify this, we mask the position of q_{i-2} in the final layer and analyze the resulting changes in probing accuracy for state q_i at the last position. The results show that after masking, the MLP11 probing score drops from above 0.9 to nearly zero, indicating that attending to q_{i-2} in the last layer is crucial for accurate state transitions at the current step. In contrast, we hold ablation experiments with a model trained without noise, and we observe minimal change in the probing accuracy for state q_i while masking. This suggests that the automaton may develop adaptive attention mechanisms to compensate for noise in the scratchpad.

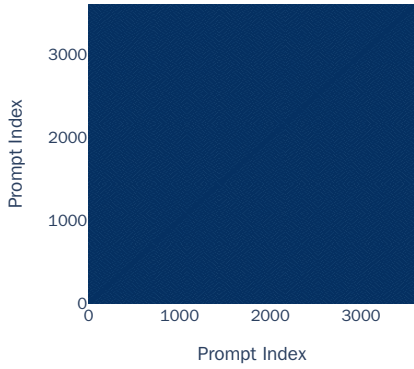
L Generalization Performance for Other Length Ranges

There are many factors contributing to weak length generalization. Here, we explain the model's failure in length generalization from the perspective of MLP neurons. We calculate neurons precision and recall (Section 4.2) on word problems with one length exceeding the training set and another below the training set. Results in Figure 10 show that neurons' precision and recall decrease sharply, with the inference step larger than the maximum length seen before. Interestingly, we have found that when

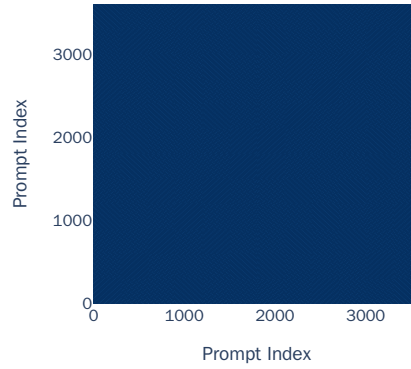
the sequence length exceeds the training data by a small margin, there is a “U-turn” phenomenon in precision during the last few steps of inference, which will yet disappear with the length increasing. To explore the “U-turn” phenomenon, we conduct experiments with models train on various length ranges and find that the margin is roughly between 125% and 150%, beyond which the phenomenon disappears. Additionally, this phenomenon also exists when the test length is slightly shorter than the training length. This may indicate that activating correct neurons is not the determining factor limiting length generalization. Finally, we conclude that improving the length generalization ability of the model requires other methods, perhaps the model structure, loss function or optimization algorithm.

Table 2: Symbols used in this paper

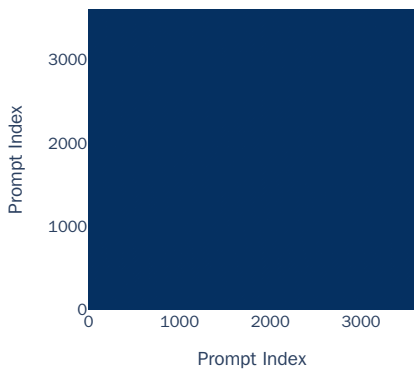
Symbol	Description
Σ	Finite set of characters
Q	Finite set of states in the automaton
q_0	Start state, an element of the state set Q
δ	State-transition function
(M, \cdot)	A monoid
M^*	Set of all possible sequences from M
m_i	The i th input of in word problems
e	The starting state
Z_m	Cyclic group of order m
S_m	Symmetric group of order m
TC^0	A complexity class in computational complexity theory, consisting of problems solvable by uniform constant-depth threshold circuits with a polynomial number of gates.
NC^1	A complexity class containing problems solvable by uniform logarithmic-depth Boolean circuits with a polynomial number of gates and bounded fan-in.
\mathbb{Z}_{60}	an abelian group encoding mod-60 addition
A_5	the alternating group on five elements
$A_4 \times \mathbb{Z}_5$	a non-abelian but solvable group
p_i	Prompt at the i th step
q_i	Result state at the i th step
\hat{q}_i	Error state
p'_i	Counterfactual prompt at the i th step
q'_i	Counterfactual result state at the i th step
P	Pre-intervention probability distribution
P^*	Post-intervention probability distribution
x^l	Input at layer l
K^l	The weight matrix at layer l
V^l	The bias vector at layer l
d_{mlp}	the MLP intermediate dimension
d_m	the model dimension
f	Non-linear activation function
k_j^l	the j -th row vectors of K^l
v_j^l	the j -th row vectors of V^l
m_j^l	Activation coefficient at the j th neuron
N_{p_i}	Set of activated neurons on prompt p_i
$N_{p'_i}$	Set of activated neurons on prompt p'_i
\mathcal{L}_{n-1}	Length of the state sequence $q_1 \dots q_{n-1}$ except last state
\mathcal{L}_n	Length of the state sequence $q_1 \dots q_n$



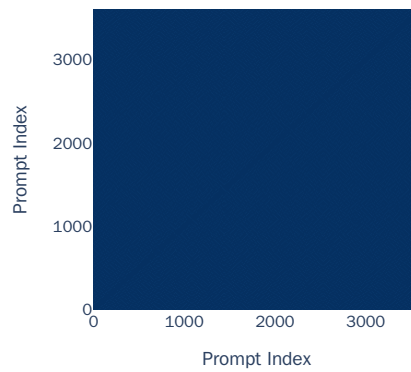
(a)



(b)



(c)



(d)

Figure 9: (a): Compression and distinction metrics for MLP10 on A_5 . (b): Compression and distinction metrics for MLP11 on $A_4 \times \mathbb{Z}_5$. (c): Compression and distinction metrics for MLP11 on \mathbb{Z}_{60} . (d): Compression and distinction metrics for MLP10 on A_5 with larger model scale. The entire square's dark color represents that the metric of any pairwise combination of prompts is nearly 1.

Model	Architecture	Task
RNN	Encoder	TT
LSTM	Encoder	TT
S4	Encoder	TT
Mamba	Encoder	TT
Transformer	Encoder	TT
Transformer+CoT	Decoder	LM
Recurrent	Encoder	TT
Looped	Encoder	TT
Pause	Decoder	LM

Table 3: Depth and time complexity of different models. TT and LM represent Token-Tagging task and Language Modeling task, respectively.

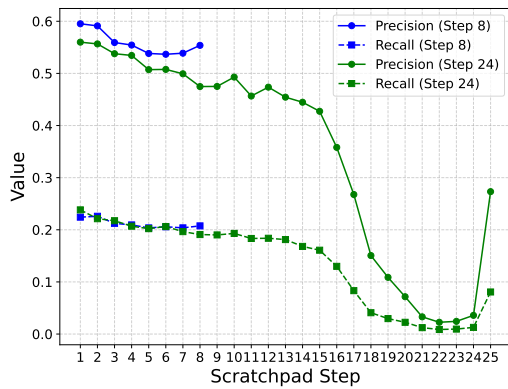


Figure 10: MLP11 neurons precision and recall across intermediate steps on A5 with length 8 and 25. The model is trained on sequences with length ranging from 10 to 20.

Group	Proper Subsets
A_5	Identity and Double Transpositions: 0, 3, 8, 11, 12, 13, 14, 27, 30, 33, 41, 43, 47, 53, 55, 59 3-Cycles: 1, 2, 4, 5, 6, 7, 9, 10, 15, 19, 22, 24, 28, 29, 37, 39, 40, 49, 51, 52 5-Cycles: 16, 17, 18, 20, 21, 23, 25, 26, 31, 32, 34, 35, 36, 38, 42, 44, 45, 46, 48, 50, 54, 56, 57, 58
$A_4 \times \mathbb{Z}_5$	Order 15: 6, 7, 8, 9, 11, 12, 13, 14, 21, 22, 23, 24, 26, 27, 28, 29, 31, 32, 33, 34, 36, 37, 38, 39, 46, 47, 48, 49, 51, 52, 53, 54 Other Orders: 0, 15, 40, 55, 5, 10, 20, 25, 30, 35, 45, 50, 1, 2, 3, 4, 16, 17, 18, 19, 41, 42, 43, 44, 56, 57, 58, 59
\mathbb{Z}_{60}	< 30: 0, 1, 2, 3, 4, 5, 6, 7, 8, 9, 10, 11, 12, 13, 14, 15, 16, 17, 18, 19, 20, 21, 22, 23, 24, 25, 26, 27, 28, 29 ≥ 30: 30, 31, 32, 33, 34, 35, 36, 37, 38, 39, 40, 41, 42, 43, 44, 45, 46, 47, 48, 49, 50, 51, 52, 53, 54, 55, 56, 57, 58, 59

Table 4: Division of elements for three groups in out-of-distribution.